symmetry

MDPI

Communication

Flavor Symmetry of Hydrogen Atoms Potentially Affecting the Proton Radius Deduced from the Electron-Hydrogen Scattering

Eugene Oks

Physics Department, Auburn University, 380 Duncan Drive, Auburn, AL 36849, USA; oksevgu@auburn.edu

Abstract: Precise knowledge of such fundamental quantity as the proton charge radius r_p is extremely important both for the quantum chromodynamics (for quark-gluon structure) and for atomic physics (for atomic hydrogen spectroscopy). Yet the ambiguity in measuring r_p persists for over a dozen of years by now—from the time when in 2010 the muonic hydrogen spectroscopy experiment yielded $r_p \approx 0.84$ fm in contrast to the form factor experiment by the Mainz group that produced $r_p \approx 0.88$ fm. Important was that this difference corresponded to about seven standard deviations and therefore was inexplicable. In the intervening dozen of years, more experiments of various kinds were performed in this regard. Nevertheless, the controversy remains, which is why several different types of new experiments are being prepared for measuring r_p. In one of our previous papers, we pointed out the factor that was never taken into account by the corresponding research community: the *flavor symmetry* of electronic hydrogen atoms, whose existence was confirmed by four kinds of atomic or molecular experiments and also evidenced by two kinds of astrophysical observations. Specifically, in that paper there was discussed the possible presence of the second flavor of muonic hydrogen atoms (in the corresponding experimental gas) and its effect on the shift of the ground state of muonic hydrogen atoms due to the proton finite size. In the present paper we analyze the effect of the *flavor symmetry* of electronic hydrogen atoms on the corresponding elastic scattering cross-section and on the proton charge radius r_p deduced from the cross-section. As an example, we use our analytical results for reconciling two distinct values of r_p obtained in different elastic scattering experiments: 0.88 fm and 0.84 fm (which is by about 4.5% smaller than 0.88 fm). We show that if the ratio of the second flavor of hydrogen atoms to the usual hydrogen atoms in the experimental gas would be about 0.3, then the extraction of r_p from the corresponding cross-section would yield by about 4.5% smaller value of r_p compared to its true value. We also derive the corresponding general formulas that can be used for interpreting the future electronic and muonic experiments.

Keywords: flavor symmetry of hydrogen atoms; proton radius; electron-hydrogen elastic scattering

Citation: Oks, E. Flavor Symmetry of Hydrogen Atoms Potentially Affecting the Proton Radius Deduced from the Electron-Hydrogen Scattering. *Symmetry* **2023**, *15*, 1760. https://doi.org/10.3390/sym15091760

Academic Editors: Stefano Profumo, Vladimir Dobrev and Sergei D. Odintsov

Received: 18 August 2023
Revised: 24 August 2023
Accepted: 11 September 2023
Published: 14 September 2023

1. Introduction

The ambiguity in measuring the proton charge radius r_p persists for over a dozen of years by now—from the time when in 2010 the muonic hydrogen spectroscopy experiment [1] yielded $r_p \approx 0.84$ fm in contrast to the form factor experiment by the Mainz group [2] that produced $r_p \approx 0.88$ fm. Important was that this difference corresponded to about seven standard deviations and therefore was inexplicable.

In the intervening dozen of years, more experiments of various kinds were performed in this regard, such as, for example, [3–9]. We also mention some of the theoretical papers providing the interpretation or reinterpretation of the experimental results, such as, for instance, [10–12]. More references on the corresponding experimental and theoretical/interpretational papers can be found, for example, in reviews [13–16], as well as in the recent presentations at the 25th European Conference on Few-Body Problems in Physics by Antognini [17], Gao [18], and Meissner [19]. Yet the problem has not been resolved yet and the controversy remains as noted, e.g., in reviews [3,14,16].

In paper [20] we pointed out the factor that was never taken into account by the corresponding research community: the *flavor symmetry* of electronic hydrogen atoms, whose existence was confirmed by four kinds of atomic or molecular experiments and also evidenced by two kinds of astrophysical observations. (In short, it is about the second solution of the standard Dirac equation for atomic hydrogen, corresponding to the same energy and the first, well-known solution: hence, the additional degeneracy; consequently, an additional conserved quantity; thus, the *flavor symmetry*—more details are provided in Appendix A). Specifically, in paper [20] there was discussed the possible presence of the second flavor of muonic hydrogen atoms (in the corresponding experimental gas) and its effect on the shift of the ground state of muonic hydrogen atoms due to the proton finite size. It was shown that even a relatively small ratio $\varepsilon \sim 0.1$ of the second flavor and usual muonic hydrogen atoms can lead to about 4% difference in the experimentally deduced parameters.

In the present paper we analyze the effect of the *flavor symmetry* of electronic hydrogen atoms on the corresponding elastic scattering cross-section and on the proton charge radius r_p deduced from the cross-section. As an example, we use our analytical results for reconciling two distinct values of r_p obtained in different experiments dealing with the elastic scattering of electrons on the electronic hydrogen atoms: the value of $r_p = 0.88$ fm from experiments [2,3,12] with the value of $r_p = 0.84$ fm from the experiment [8], which is by about 4.5% smaller than 0.88 fm. (To give an idea of the experimental parameters, we mention that, e.g., in experiment [8] the electron beams had the energy of either 1.1 GeV or 2.2 GeV, and the angular acceptance of the hybrid calorimeter was from 0.7 degrees to 7.0 degrees.) Also, we provide the corresponding general formulas that can be used for interpreting the future electronic and muonic experiments.

2. Model

In paper [20], based on the analytical results of paper [21], it was shown that if a share ε of the second flavor of *muonic* hydrogen atoms is present in the experimental muonic hydrogen gas, then it affects the shift of energy of the ground state ΔE caused by the finite size of the proton in the following way:

$$\Delta E(\varepsilon, R_p) = b(16\beta^{3/2}){R_p}^2[1/{R_p}^{\beta} - \varepsilon R_p/(5\beta) + \varepsilon^2 {R_p}^2/(100\beta^2)]. \quad (1)$$

In that equation, ε was the share of the second flavor of muonic atoms in the muonic hydrogen gas and it was considered relatively small ($\varepsilon << 1$); R_p was the proton radius calculated in units of the muonic Bohr radius $a_{0\mu} = \hbar^2/(m_\mu e^2)$; $\beta = \alpha^2 << 1$ (α being the fine structure constant); b was a constant of no significance for the goal of paper [20].

In the present paper we consider how the shift of the ground state energy ΔE of *electronic* hydrogen atoms due to the proton finite size and the corresponding elastic scattering cross-section are affected by the presence of the second flavor of *electronic* hydrogen atoms in the experimental hydrogen gas in the ratio ε to the usual hydrogen atoms. We note that here the restriction $\varepsilon << 1$ is not imposed.

Below we call the space outside the proton as the exterior and the space inside the proton as the interior. For the ground state of *electronic* atomic hydrogen in the exterior, the radial part of the Dirac bispinor, based on Equation (17) from paper [21], can be written as follows:

$$\begin{aligned} f(r) &\approx -2\beta^{5/4}\{1/r^{\beta/2} - \varepsilon[{R_p}^2/(5\beta r^{2-\beta/2})]\}/(1+\varepsilon^2)^{1/2}, \\ g(r) &\approx 4\beta^{3/4}\{1/r^{\beta/2} - \varepsilon[{R_p}^2/(10\beta r^{1-\beta/2})]\}/(1+\varepsilon^2)^{1/2}. \end{aligned} \quad (2)$$

Here R_p is the proton "sphere" radius, that is, the borderline between the singular solution of the Dirac equation in the exterior and the regular solution of the Dirac equation in the interior. The proportionality relation between the proton charge radius r_p and R_p is specified later on. (In Equation (2), compared to the corresponding Equation (2) from paper [20], we entered the normalizing factor $(1+\varepsilon^2)^{1/2}$, as the denominator.)

After following the same sequence of steps as in paper [20], the shift of the energy of the ground state ΔE caused by the finite size of the proton can be written similarly to Equation (1), but with the denominator $(1 + \varepsilon^2)$ and with the rescaled value of the proton "sphere" radius R_p—namely, now R_p is in units of the *electronic* Bohr radius $a_{0e} = \hbar^2/(m_e e^2)$:

$$\Delta E(\varepsilon, R_p) = \text{const}\, {R_p}^2[1/{R_p}^\beta - \varepsilon R_p/(5\beta) + \varepsilon^2 {R_p}^2/(100\beta^{2+\beta})]/(1 + \varepsilon^2). \quad (3)$$

In Equation (3), the energy is expressed in atomic units ($\hbar = m_e = e = 1$).

Next, we estimate the relation between the relative change $\delta\sigma = \Delta\sigma/\sigma$ of the cross-section for the electron-hydrogen elastic scattering and the relative shift $\delta E = \Delta E/E$ of the ground state energy caused by the admixture of the second flavor of hydrogen atoms. For our simple model, intended just for getting the message across, for the cross-section of the elastic scattering in the case of relatively low values of the momentum transfer, which is relevant to deducing the proton radius from the electron-hydrogen scattering—we use the relation

$$\sigma = \text{const}\, (<r^2>)^2, \quad (4)$$

taken from Equation (115.4) from the textbook [22]. In Equation (4), r is the distance of the atomic electron from the proton; the symbol <. . .> stands for "averaged".

The unperturbed binding energy of the atomic electron (i.e., for $\varepsilon = 0$) in the ground state E_b (or in any state) of hydrogen atoms is inversely proportional to $(<r^2>)$:

$$E_b = \text{const}/(<r^2>), \quad (5)$$

so that

$$(<r^2>) = \text{const}/E_b. \quad (6)$$

Consequently,

$$|\,\delta(<r^2>)\,| = |\,\delta E_b\,|, \quad (7)$$

where

$$\delta(<r^2>) = \Delta(<r^2>)/(<r^2>),\ \delta E_b = \Delta E_b/E_b. \quad (8)$$

From Equation (4) it follows that

$$\delta\sigma = \Delta\sigma/\sigma = 2\,\delta(<r^2>), \quad (9)$$

where σ is the corresponding cross-section at $\varepsilon = 0$. Then combining Equation (9) with Equation (7) we obtain:

$$|\,\delta\sigma(\varepsilon, R_p)\,| = 2\,|\,\delta E_b(\varepsilon, R_p)\,|. \quad (10)$$

Since the unperturbed cross-section σ and the unperturbed binding energy E_b do not depend on ε, then the change of the cross-section $\Delta\sigma$ has the same dependence on ε as ΔE from Equation (3) (apart from a constant)

$$\Delta\sigma(\varepsilon, R_p) = \text{const}\, {R_p}^2[1/{R_p}^\beta - \varepsilon R_p/(5\beta) + \varepsilon^2 {R_p}^{2+\beta}/(100\beta^2)]/(1 + \varepsilon^2). \quad (11)$$

Some electron scattering experiments yielded the proton radius charge $r_p = 0.88$ fm [2,3,12], while another electron scattering experiment yielded $r_p = 0.84$ fm [8], that is, by about 4.5% less than 0.88 fm. Therefore, we will seek the value of ε, such that

$$\Delta\sigma(\varepsilon, R_p) = \Delta\sigma(0, 0.955R_p). \quad (12)$$

In other words, the purpose of solving Equation (12) is to show that from the same experimental cross-section, one can find either the smaller value of R_p while neglecting a possible admixture of the second flavor of hydrogen atoms to the experimental hydrogen gas (i.e., at $\varepsilon = 0$) or by 4.5% larger value of R_p at some finite value of ε.

Equation (12), being quadratic with respect to ε, has the following two solutions:

$$\varepsilon_1 = [7.50 \times 10^7 R_p - (1.284 + 5.14 \times 10^{15} {R_p}^2)^{1/2}]/(1.408 \times 10^{11} {R_p}^2 - 3.65 \times 10^4), \quad (13)$$

$$\varepsilon_2 = [7.50 \times 10^7 R_p + (1.284 + 5.14 \times 10^{15} {R_p}^2)^{1/2}]/(1.408 \times 10^{11} {R_p}^2 - 3.65 \times 10^4). \quad (14)$$

For numerically estimating the share of the second flavor of hydrogen atoms in the experimental hydrogen gas, we use for the proton charge radius r_p the value of 0.86 fm, which is the mean value between 0.88 fm and 0.86 fm. After the conversion into the atomic units, we obtain $r_p = 0.0000163$.

The proton "sphere" radius R_p would be by the factor of $(5/3)^{1/2}$ larger than r_p (it would be equal to 0.0000210) in the model of the proton as a uniformly charged sphere (what the proton is not). The actual value of R_p should be between 0.0000163 and 0.0000210. For numerical evaluations of ε_1 and ε_2, if we assume the value $R_p \approx 0.000018$, then

$$\varepsilon_1 \approx 0.276, \varepsilon_2 \approx -0.350 \quad (15)$$

(obviously, the negative value of ε_2 is non-physical). As for ε_1, more precisely, the interval $0.0000163 < R_p < 0.0000210$ yields $0.271 < \varepsilon_1 < 0.280$.

Due to the proportionality between the proton charge radius r_p and the proton "sphere" radius R_p, the above qualitative and quantitative result for the dependence of R_p, deduced from the elastic cross-section, on the share of the second flavor of hydrogen atoms in the experimental hydrogen gas, is also the same for r_p. In other words, about 30% ratio of the second flavor of hydrogen atoms to the usual hydrogen atoms in the experimental gas can precipitate the conclusion that r_p is by 4.5% lesser than its true value.

For interpreting future experiments on the elastic scattering of electrons or muons on the atomic hydrogen, we consider below the general equation

$$\Delta\sigma(\varepsilon, R_p) = \Delta\sigma[0, (1 - a)R_p], \quad (16)$$

where a is the relative discrepancy between the values of the proton charge radius deduced from different experiments. (For example, in Equation (12), a was entered as 0.045.) The solutions of the quadratic Equation (16) are as follows:

$$\begin{aligned} \varepsilon_1 &= \{[1.408 \times 10^7 {R_p}^2 + 4a(2 - a)(1 - 2a - a^2 - 3.52 \times 10^6 {R_p}^2)]^{1/2} - 3.75 \times 10^3 R_p\}/[2(1 - 2a - a^2 - 3.52 \times 10^6 {R_p}^2)], \\ \varepsilon_2 &= \{-[1.408 \times 10^7 {R_p}^2 + 4a(2 - a)(1 - 2a - a^2 - 3.52 \times 10^6 {R_p}^2)]^{1/2} - 3.75 \times 10^3 R_p\}/[2(1 - 2a - a^2 - 3.52 \times 10^6 {R_p}^2)]. \end{aligned} \quad (17)$$

Only the solution ε_1 is physically admissible: the solution ε_2 is negative and thus physically inadmissible.

Figure 1 illustrates the dependence of ε_1 on a and R_p.

Figure 2 shows the same as Figure 1, but from another viewpoint, so that together with Figure 1 it provides more comprehensive understanding of dependence of ε_1 on a and R_p.

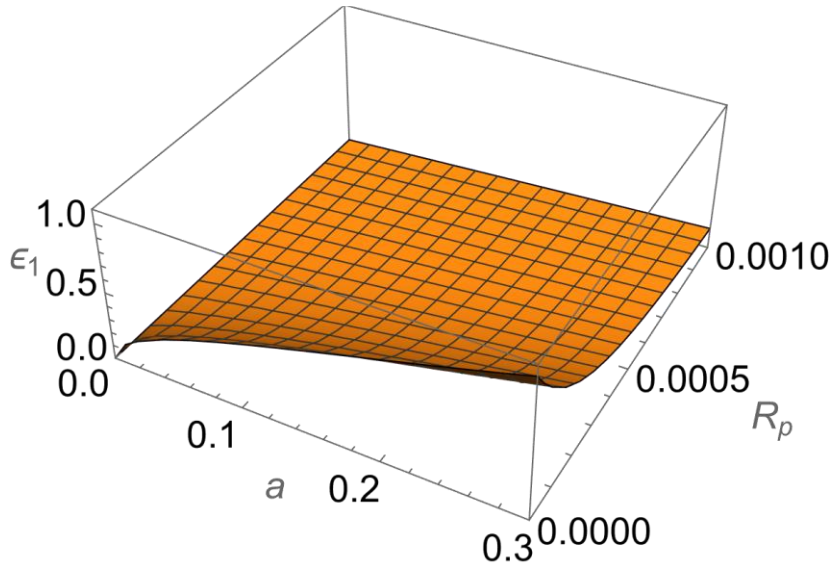

Figure 1. The dependence of the ratio ε_1 of the second flavor hydrogen atoms to the usual hydrogen atoms (required for reconciling the relative difference a between the values of the proton charge radius r_p deduced from various experiments) on the value of a and on the proton "sphere" radius R_p (proportional to r_p).

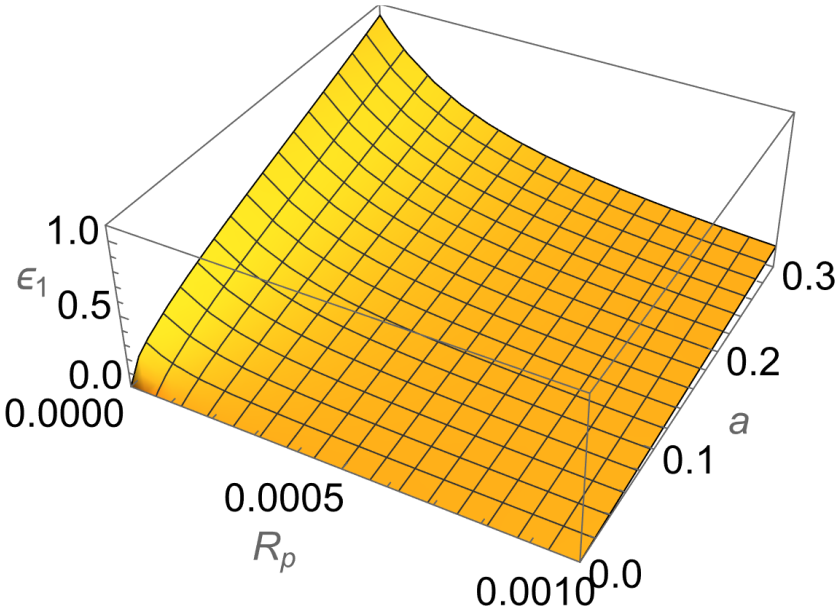

Figure 2. The same as on Figure 1, but from another viewpoint.

3. Conclusions

We presented a relatively simple model demonstrating how the *flavor symmetry* of hydrogen atoms affects the value of the proton charge radius r_p deduced from the experimental results on the elastic scattering of electrons. We provided the corresponding general formulas that can be used for interpreting the future electronic and muonic experiments.

As an example, we applied our analytical results for reconciling two distinct values of r_p obtained in different experiments on the elastic scattering of electrons on the electronic hydrogen atoms: the value of r_p = 0.88 fm from experiments [2,3,12] with the value of r_p = 0.84 fm from the experiment [8] (which is by about 4.5% smaller than 0.88 fm). We demonstrated that if the ratio of the second flavor of hydrogen atoms to the usual hydrogen atoms in the experimental gas would be about 0.3, then the extraction of r_p from the

corresponding cross-section would yield by about 4.5% smaller value of r_p compared to its true value.

We do not imply that this relatively simple model is the ultimate resolution of the controversy. The intent of our paper is to stimulate further theoretical/interpretational studies in this fundamental research field—especially in view of the planned scattering experiments, such as, e.g., MUSE [23], PRad-II [24,25], COMPASS++/AMBER [26], and ULQ2 [27].

Funding: This research received no external funding.

Data Availability Statement: All data is included in the paper.

Acknowledgments: The author is grateful to A. Antognini and to H. Gao for illuminating discussions during the 25th European Conference on Few-Body Problems in Physics.

Conflicts of Interest: The author declares no conflict of interest.

Appendix A. Brief Overview of the Atomic/Molecular Experiments and Astrophysical Observations Proving the Existence of the Flavor Symmetry of Hydrogen Atoms

There are two analytical solutions of the standard Dirac equation for atomic hydrogen: (1) the weakly singular at small r (called "regular"); (2) the strongly singular at small r (called "singular"). For the 2nd solution the normalization integral diverges at small r, which is why this solution is usually rejected. Even after taking into account that the proton has the finite size but modeling the charge distribution inside the proton as that of a uniformly charged sphere or of a uniform spherical shell, the singular solution outside the proton did not work.

In paper [21] there was discovered a general class of interior potentials (i.e., the potentials inside the nucleus), for which the singular solution outside the nucleus can be in fact matched with the corresponding regular interior solution (i.e., inside the nucleus). This class of potentials included, in particular, those corresponding to the charge distributions that have the maximum at r = 0. In the well-known experiments, where electrons were elastically scattered on protons (see, e.g., paper [28] and book [29]), it was found that inside protons, the charge distribution does have the maximum at r = 0. In papers [21,30] it was shown that for the true charge distribution inside the proton, the regular interior solution can be matched with the singular exterior solution for any $l = 0$ state of the discrete and continuous spectrum: the singular solution of the standard Dirac equation for hydrogen atoms is legitimate for all S-states.

Both the regular and singular solutions for the wave functions in the exterior correspond to *the same energy*. Thus, there is an *additional degeneracy*. Consequently, in accordance to the well-known theorem of quantum mechanics, hydrogen atoms should have an *additional conserved quantity*. So, hydrogen atoms have two flavors that are distinguish by the eigenvalue of this conserved quantity. In other words, hydrogen atoms possess the *flavor symmetry* [31]. It is named so by analogy with the flavor symmetry of quarks. This is why the second type of hydrogen atoms having only the S-states was named the Second Flavor of Hydrogen Atoms (SFHA).

By virtue of having only the S-states, the SFHA do not couple to the electromagnetic radiation according to the quantum-mechanical selection rules (except the coupling between the two hyperfine sublevels of the ground state resulting in the 21 cm spectral line): *the SFHA are dark*. This is true for any multipole radiation (rather than only for the dipole radiation), as well as for multi-photon transitions.

By now the presence of the SFHA is confirmed by the following four different kinds of atomic or molecular experiments.

1. Experimental High-energy Tail of the linear Momentum Distribution (HTMD) in the ground state of atomic hydrogen.

The HTMD, determined by analyzing atomic experiments for a large set of different collisional processes between hydrogen atoms and protons or electrons, was found to fall

off much more slowly [32] than the theoretical HTLMD [33]. *The discrepancy was several thousand times*.

In paper [21] it was demonstrated that with the allowance for the SFHA, this huge discrepancy got completely removed. This was due to the fact that for the singular exterior solution, a much more rapid increase of the wave function in the direction to the proton at small r corresponds to a *much slower decline* of the wave function in the p-representation for large p (as follows from the properties of the Fourier transform).

2. Experiments on the excitation of *atomic* hydrogen by the electron impact.

The experimental ratio σ_{2s} to σ_{2p}, where σ_{2s} and σ_{2p} are the cross-sections of the excitation to the states 2s and 2p, respectively, was by about 20% larger [34] than the corresponding theoretical ratio [35]. This discrepancy was significantly higher than the experimental error margins of 9%.

The experimental cross-section σ_{2s} was deduced by using the quenching technique: by subjecting the system to an electric field that intermixed the state 2s and 2p, and then registering the emission of the Lyman-alpha line (i.e., the radiative transition from the state 2p to the ground state). The main point is the following. In the mixture of the SFHA with the usual hydrogen atoms, both flavors can be excited to the 2s state. However, the mixing of the 2s and 2p states by the electric field happens only for the usual hydrogen atoms: the SFHA, due to having only the S-states, cannot not make any contribution to the observed Lyman-alpha signal.

For this reason, measuring the cross-section σ_{2s} in this manner, should underestimates σ_{2s} compared to its true value, while the cross-section σ_{2p} would not be influenced by the presence of the SFHA. In paper [36] it was shown that the above can be eliminated if the SFHA were present in the share ~40% in the experimental hydrogen gas. Again, no alternative explanation was ever provided.

3. Experiments on the excitation of *molecular* hydrogen by the electron impact.

For the excitation of the first two stable excited electronic triplet states of H_2—$c^3\Pi_u$ and $a^3\Sigma_g^+$—even the most advanced calculations by the convergent close-coupling method employing 491 states [37] underestimate the experimental cross-sections ([38,39] by *at least a factor of two*.

In paper [40] it was shown the following. If in the molecular hydrogen gas, for some molecules one or both atoms would be the SFHA, then the above very large discrepancy would be removed. The reason is the following. For such unusual H_2 molecules, the corresponding theoretical cross-section is by a factor of three greater than for the usual H_2 molecules. The presence of about 30% of the SFHA-based H_2 molecules in the experimental gas would suffice for removing the above discrepancy.

4. Experiments on the charge exchange between low energy protons incident on hydrogen atoms

The experimental cross-sections [41] were noticeably greater than the theoretical ones calculated in paper [42]. Again, this discrepancy can be removed if there was the presence of the SFHA in the experimental gas [43]. The reason is the following.

The cross-section for the resonant charge exchange is (roughly) inversely proportional to the square of the ionization potential U_{ioniz} from the particular atomic state. For the usual hydrogen atoms, U_{ioniz} increases due to the Stark shift by the field of the incoming proton. However, for the SFHA there is no shift of the energy levels by the electric field.

There were never given any alternative (to the SFHA) explanation of the above discrepancies for any of the above experiments.

There are also two types of the astrophysical evidence of the SFHA presence.

1. Baffling observation of the cosmologically redshifted 21 cm spectral line from the early Universe.

The observed absorption in this cosmologically redshifted line was found to be *two times more intense* than expected from the standard cosmology [44]. The ramification was that *the gas temperature* of the hydrogen *was actually significantly lesser* than expected from the standard cosmology.

Barkana [45] hypothesized that some unspecified dark matter had collisions with the hydrogen gas and decreased its temperature compared to the expectations of the standard cosmology. He found out that for thev quantitative explanation of the observations, the mass of these dark matter particles should be of the same order as protons, or neutrons, or hydrogen atoms. In paper [30] the following scenario was analyzed: what if Barkana's unspecified dark matter particles are the SFHA?

The SFHA couples to the radiative transitions between the two hyperfine sublevels of the ground state just as the usual hydrogen atoms. In paper [30] it was expounded that in the course of the Universe expansion, the SFHA (due to having only S-states) decouple from the Cosmic Microwave Background (CMB) radiation earlier than the usual hydrogen atoms. Therefore, the SFHA cool down more rapidly than the usual hydrogen atoms (which decouple from the CMB radiation significantly later). For this reason, the spin temperature (which controls the intensity of the absorption signal in the 21 cm line) was smaller for the SFHA. In paper [30] it was shown that this explains the observed anomaly in the absorption in the 21 cm line both *qualitatively and quantitatively*.

2. Observed anomalous distribution of dark matter in the Universe.

It was found to be smoother, less clumpy than predicted by general relativity [46], what caused calls for new physical laws. However, in paper [47] it was shown that this baffling observation can be also expounded *qualitatively and quantitatively* on the basis of the SFHA—without resorting to new physical laws.

The above SFHA-based explanations of these two puzzling astrophysical observations made the SFHA one of the leading candidates for dark matter or for a part of it—see, e.g., review [48]. As for future atomic experiments, we could suggest a different kind that could yield yet another evidence of the presence of the SFHA: namely, the experiments on the formation of H_2^+ by collision of protons with hydrogen atoms. We predict due to the SFHA, the *relative intensity* of the band, resulting from the radiative transitions between the terms $5f\sigma$ and $4d\sigma$ of H_2^+, would be significantly higher compared to the absence of the SFHA.

References

1. Pohl, R.; Antognini, A.; Nez, F.; Amaro, F.D.; Biraben, F.; Cardoso, J.M.; Kottmann, F. The Size of the Proton. *Nature* **2010**, *466*, 213–216. [CrossRef]
2. Bernauer, J.C.; Achenbach, P.; Gayoso, C.A.; Böhm, R.; Bosnar, D.; Debenjak, L.; Distler, M.O.; Doria, L.; Esser, A.; Fonvieille, H.; et al. High-Precision Determination of the Electric and Magnetic Form Factors of the Proton. *Phys. Rev. Lett.* **2010**, *105*, 242001. [CrossRef]
3. Zhan, X.; Allada, K.; Armstrong, D.; Arrington, J.; Bertozzi, W.; Boeglin, W.; Chen, J.-P.; Chirapatpimol, K.; Choi, S.; Chudakov, E.; et al. High-Precision Measurement of the Proton Elastic Form Factor Ratio $\mu_p G_E/G_M$ at Low Q^2. *Phys. Lett. B* **2011**, *705*, 59–64. [CrossRef]
4. Antognini, A.; Nez, F.; Schuhmann, K.; Amaro, F.D.; Biraben, F.; Cardoso, J.M.R.; Covita, D.S.; Dax, A.; Dhawan, S.; Diepold, M.; et al. Proton structure from the measurement of 2S-2P transition frequencies of muonic hydrogen. *Science* **2013**, *339*, 417–420. [CrossRef] [PubMed]
5. Mihovilovič, M.; Weber, A.; Achenbach, P.; Beranek, T.; Beričič, J.; Bernauer, J.; Böhm, R.; Bosnar, D.; Cardinali, M.; Correa, L.; et al. First Measurement of Proton's Charge Form Factor at Very Low Q^2 with Initial State Radiation. *Phys. Lett. B* **2017**, *771*, 194–198. [CrossRef]
6. Fleurbaey, H.; Galtier, S.; Thomas, S.; Bonnaud, M.; Julien, L.; Biraben, F.; Guéna, J. New Measurement of the 1S–3S Transition Frequency of Hydrogen: Contribution to the Proton Charge Radius Puzzle. *Phys. Rev. Lett.* **2018**, *120*, 183001. [CrossRef] [PubMed]
7. Bezginov, N.; Valdez, T.; Horbatsch, M.; Marsman, A.; Vutha, A.C.; Hessels, E.A. A measurement of the atomic hydrogen Lamb shift and the proton charge radius. *Science* **2019**, *365*, 1007–1012. [CrossRef]
8. Xiong, W.; Gasparian, A.; Gao, H.; Dutta, D.; Khandaker, M.; Liyanage, N.; Pasyuk, E.; Peng, C.; Bai, X.; Ye, L.; et al. A small proton charge radius from an electron–proton scattering experiment. *Nature* **2019**, *575*, 147–151. [CrossRef]
9. Brandt, A.D.; Cooper, S.F.; Rasor, C.; Burkley, Z.; Matveev, A.; Yost, D.C. Measurement of the $2S_{1/2}$–$8D_{5/2}$ Transition in Hydrogen. *Phys. Rev. Lett.* **2022**, *128*, 023001. [CrossRef]
10. Sick, I. Problems with Proton Radii. *Progr. Part. Nucl. Phys.* **2012**, *67*, 473–478. [CrossRef]
11. Lee, G.; Arrington, J.R.; Hill, R.J. Extraction of the Proton Radius from Electron-Proton Scattering Data. *Phys. Rev. D* **2015**, *92*, 013013. [CrossRef]

12. Mihovilovič, M.; Achenbach, P.; Beranek, T.; Beričič, J.; Bernauer, J.C.; Böhm, R.; Bosnar, D.; Cardinali, M.; Correa, L.; Debenjak, L.; et al. The Proton Charge Radius Extracted from the Initial-State Radiation Experiment at MAMI. *Eur. Phys. J. A* **2021**, *57*, 107. [CrossRef]
13. Karr, J.P.; Marchand, D. Progress on the proton radius puzzle. *Nature* **2019**, *575*, 61–62. [CrossRef] [PubMed]
14. Bernauer, J.C. The Proton Radius Puzzle—9 Years Later. *EPJ Web Conf.* **2020**, *234*, 01001. [CrossRef]
15. Pacetti, S.; Tomasi-Gustafsson, E. The Origin of the Proton Radius Puzzle. *Eur. Phys. J. A* **2021**, *57*, 72. [CrossRef]
16. Gao, H.; Vanderhaenghen, M. The Proton Charge Radius. *Rev. Mod. Phys.* **2022**, *94*, 015002. [CrossRef]
17. Antognini, A. Precision Benchmarks for Nuclear and Atomic Physics from Laser Spectroscopy of Muonic Atoms. In Proceedings of the 25th European Conference on Few-Body Problems in Physics, Mainz, Germany, 30 July–4 August 2023; Available online: https://indico.him.uni-mainz.de/event/150/contributions/1128/ (accessed on 18 August 2023).
18. Gao, H. Recent Results on Proton Charge Radius and Polarizabilities. In Proceedings of the 25th European Conference on Few-Body Problems in Physics, Mainz, Germany, 30 July–4 August 2023; Available online: https://indico.him.uni-mainz.de/event/150/contributions/1135/ (accessed on 18 August 2023).
19. Meißner, U.-G. The Proton Radius and its Relatives A.D. In Proceedings of the 25th European Conference on Few-Body Problems in Physics, Mainz, Germany, 30 July–4 August 2023; Available online: https://indico.him.uni-mainz.de/event/150/contributions/1148/ (accessed on 18 August 2023).
20. Oks, E. A Possible Explanation of the Proton Radius Puzzle based on the Second Flavor of Muonic Hydrogen Atoms. *Foundations* **2022**, *2*, 912–917. [CrossRef]
21. Oks, E. High-Energy Tail of the Linear Momentum Distribution in the Ground State of Hydrogen Atoms or Hydrogen-like Ions. *J. Phys. B At. Mol. Opt. Phys.* **2001**, *34*, 2235–2243. [CrossRef]
22. Landau, L.D.; Lifshitz, E.M. *Quantum Mechanics*; Pergamon: Oxford, UK, 1965.
23. Kohl, M. Lepton Universality Test with MUSE at PSI. *J. Phys. Conf. Ser.* **2022**, *2391*, 012015. [CrossRef]
24. Gasparian, A.; Gao, H.; Dutta, D.; Liyanage, N.; Pasyuk, E.; Higinbotham, D.W.; Peng, C.; Gnanvo, K.; Xiong, W.; Bai, X.; et al. PRad-II: A New Upgraded High Precision Measurement of the Proton Charge Radius. 2020. Available online: https://arxiv.org/abs/2009.10510 (accessed on 18 August 2023).
25. Lin, Y.-H.; Hammer, H.-W.; Meißner, U.-G. Differential Cross Section Predictions for PRad-II from Dispersion Theory. *Phys. Lett. B* **2022**, *827*, 136981. [CrossRef]
26. Adams, B.; Aidala, C.A.; Akhunzyanov, R.; Alexeev, G.D.; Alexeev, M.G.; Amoroso, A.; Makarenko, V. Letter of Intent: A New QCD Facility at the M2 Beam Line of the CERN SPS COMPASS++/AMBER. 2019. Available online: https://arxiv.org/abs/1808.00848 (accessed on 18 August 2023).
27. Suda, T. Low-Energy Electron Scattering Facilities in Japan. *J. Phys. Conf. Ser.* **2022**, *2391*, 012004. [CrossRef]
28. Simon, G.; Schmitt, C.H.; Borkowski, F.; Walther, V.H. Absolute electron-proton cross sections at low momentum transfer measured with a high pressure gas target system. *Nucl. Phys.* **1980**, *A333*, 381. [CrossRef]
29. Perkins, D.H. *Introduction to High Energy Physics*; Addison-Wesley: Menlo Park, CA, USA, 1987; Section 6.5.
30. Oks, E. Alternative Kind of Hydrogen Atoms as a Possible Explanation of the Latest Puzzling Observation of the 21 cm Radio Line from the Early Universe. *Res. Astron. Astrophys.* **2020**, *20*, 109. [CrossRef]
31. Oks, E. Two Flavors of Hydrogen Atoms: A Possible Explanation of Dark Matter. *Atoms* **2020**, *8*, 33. [CrossRef]
32. Gryzinski, M. Classical Theory of Atomic Collisions. I. Theory of Inelastic Collisions. *Phys. Rev.* **1965**, *138*, A336. [CrossRef]
33. Fock, V. Zur Theorie des Wasserstoffatoms. *Z. Phys.* **1935**, *98*, 145. [CrossRef]
34. Callaway, J.; McDowell, M.R.C. What We do and do not Know About Electron Impact Excitation of Atomic Hydrogen. *Comments At. Mol. Phys.* **1983**, *13*, 19.
35. Whelan, C.T.; McDowell, M.R.C.; Edmunds, P.W. Electron Impact Excitation of Atomic Hydrogen. *J. Phys. B At. Mol. Phys.* **1987**, *20*, 1587–1598. [CrossRef]
36. Oks, E. Experiments on the Electron Impact Excitation of the 2s and 2p States of Hydrogen Atoms Confirm the Presence of their Second Flavor as the Candidate for Dark Matter. *Foundations* **2022**, *2*, 541–546. [CrossRef]
37. Zammit, M.C.; Savage, J.S.; Fursa, D.V.; Bray, I. Electron-Impact Excitation of Molecular Hydrogen. *Phys. Rev. A* **2017**, *95*, 022708. [CrossRef]
38. Wrkich, J.; Mathews, D.; Kanik, I.; Trajmar, S.; Khakoo, M.A. Differential Cross-Sections for the Electron Impact Excitation of the B $^1\Sigma_u^+$, c $^3\Pi_u$, a $^3\Sigma^+$, C $^1\Pi_u$, E, F $^1\Sigma^+$ and e $^3\Sigma_u^+$ States of Molecular Hydrogen. *J. Phys. B At. Mol. Opt. Phys.* **2002**, *35*, 4695–4709. [CrossRef]
39. Mason, N.J.; Newell, W.R. The Total Excitation Cross Section of the c $^3\Pi_u$ State of H_2. *J. Phys. B At. Mol. Opt. Phys.* **1986**, *19*, L587–L591. [CrossRef]
40. Oks, E. Experiments on the Electron Impact Excitation of Hydrogen Molecules Indicate the Presence of the Second Flavor of Hydrogen Atoms. *Foundations* **2022**, *2*, 697–703. [CrossRef]
41. Fite, W.L.; Smith, A.C.H.; Stebbings, R.F. Charge Transfer in Collisions Involving Symmetric and Asymmetric Resonance. *Proc. R. Soc.* **1962**, *A268*, 527–536.
42. Dalgarno, A.; Yadav, H.N. Electron Capture II: Resonance Capture from Hydrogen Atoms by Slow Protons. *Proc. Phys. Soc.* **1953**, *A66*, 173. [CrossRef]

43. Oks, E. Analysis of Experimental Cross-Sections of Charge Exchange between Hydrogen Atoms and Protons Yields another Evidence of the Existence of the Second Flavor of Hydrogen Atoms. *Foundations* **2021**, *1*, 265–270. [CrossRef]
44. Bowman, J.D.; Rogers, A.E.E.; Monsalve, R.A.; Mozdzen, T.J.; Mahesh, N. An Absorption Profile Centred at 78 Megahertz in the Sky-Averaged Spectrum. *Nature* **2018**, *555*, 67–70. [CrossRef]
45. Barkana, R. Possible Interaction between Baryons and Dark-Matter Particles Revealed by the First Stars. *Nature* **2018**, *555*, 71–74. [CrossRef]
46. Jeffrey, N.; Gatti, M.; Chang, C.; Whiteway, L.; Demirbozan, U.; Kovacs, A.; Pollina, G.; Bacon, D.; Hamaus, N.; Kacprzak, T.; et al. Dark Energy Survey Year 3 results: Curved-sky weak lensing mass map reconstruction. *Mon. Not. R. Astron. Soc.* **2021**, *505*, 4626–4645. [CrossRef]
47. Oks, E. DES Map Shows a Smoother Distribution of Matter than Expected: A Possible Explanation. *Res. Astron. Astrophys.* **2021**, *21*, 241–245. [CrossRef]
48. Oks, E. Review of Latest Advances on Dark Matter from the Viewpoint of the Occam Razor Principle. *New Astron. Rev.* **2023**, *96*, 101673. [CrossRef]